



A potent neutralizing and protective antibody against a conserved continuous epitope on HSV glycoprotein D

Rui Tian^{a,1}, Fei Ju^{a,1}, Mengqin Yu^{a,1}, Zhiqi Liang^b, Zilong Xu^a, Min Zhao^b, Yaning Qin^a, Yanhua Lin^a, Xiaoxuan Huang^a, Yating Chang^b, Shaopeng Li^a, Wenfeng Ren^a, Chaolong Lin^a, Ningshao Xia^a, Chenghao Huang^{a,*}

^a State Key Laboratory of Molecular Vaccinology and Molecular Diagnostics, National Institute of Diagnostics and Vaccine Development in Infectious Diseases, School of Public Health, Xiamen University, Xiamen, Fujian, 361102, China

^b School of Life Sciences, Xiamen University, Xiamen, Fujian, 361102, China



ARTICLE INFO

Keywords:

Herpes simplex virus
Neutralizing antibody
Glycoprotein D
Nectin-1
Conserved continuous epitope

ABSTRACT

Infections caused by herpes simplex virus type 1 (HSV-1) and type 2 (HSV-2) remain a serious global health issue, and the medical countermeasures available thus far are limited. Virus-neutralizing monoclonal antibodies (NAbs) are crucial tools for studying host-virus interactions and designing effective vaccines, and the discovery and development of these NAbs could be one approach to treat or prevent HSV infection. Here, we report the isolation of five HSV NAbs from mice immunized with both HSV-1 and HSV-2. Among these were two antibodies that potently cross-neutralized both HSV-1 and HSV-2 with the 50% virus-inhibitory concentrations (IC_{50}) below 200 ng/ml, one of which (4A3) exhibited high potency against HSV-2, with an IC_{50} of 59.88 ng/ml. 4A3 neutralized HSV at the prebinding stage and prevented HSV infection and cell-to-cell spread. Significantly, administration of 4A3 completely prevented weight loss and improved survival of mice challenged with a lethal dose of HSV-2. Using structure-guided molecular modeling combined with alanine-scanning mutagenesis, we observed that 4A3 bound to a highly conserved continuous epitope (residues 216 to 220) within the receptor-binding domain of glycoprotein D (gD) that is essential for viral infection and the triggering of membrane fusion. Our results provide guidance for developing NAb drugs and vaccines against HSV.

1. Introduction

Herpes simplex virus (HSV) is a ubiquitous human pathogen, and it is categorized into two types: HSV type 1 (HSV-1) and HSV type 2 (HSV-2). Infection with different types of HSV can cause different symptoms; HSV-1 mainly causes oral herpes (including symptoms known as “cold sores”), transmitted by mouth-to-mouth contact, and it also carries the risk of genital herpes, while HSV-2 is a common sexually transmitted pathogen that causes the most prevalent form of genital herpes (Fatahzadeh and Schwartz, 2007; Whitley and Roizman, 2001). Both types of HSV virus can cause latent infections in innervating ganglia, which can carry the virus for a lifetime (Knipe and Cliffe, 2008; Steiner, 1996; Wang et al., 2012). According to the latest report from the World Health Organization (WHO) in 2016, approximately 3.7 billion people under the age of 50 had HSV-1 infection globally, and approximately 491

million people aged 15–49 years worldwide were living with HSV-2 infection (James et al., 2020). Thus, diseases caused by HSV infection, especially HSV-2, have become a global health issue (Johnston and Corey, 2016). Although several prevention and treatment measures against HSV infection have been developed in recent years, neonatal herpes infection still has an unacceptably high mortality rate, and survivors experience painful sequelae (Poole and Kimberlin, 2018). Moreover, HSV-2 can cause high morbidity and mortality in immunocompromised individuals, particularly those infected with HIV (Johnston and Corey, 2016).

Idoxuridine was used as the first antiviral agent against HSV infection in 1962 (Kaufman, 1962). However, the drug was restricted to only topical use because of the serious toxic side effects of systemic administration (Boston Interhospital Virus Study and Study, 1975). Acyclovir, famciclovir, and valacyclovir are relatively safe and efficacious oral

* Corresponding author. School of Public Health, Xiamen University, Xiang'An South Road, Xiamen, Fujian, 361102, China.

E-mail address: huangchenghao@xmu.edu.cn (C. Huang).

¹ These authors contributed equally to this work and are co-first authors.

antiviral agents that are now available for the treatment of primary genital herpes (Corey et al., 2004; Kimberlin et al., 2011; Poole and Kimberlin, 2018). These medications exert their antiviral effect by becoming incorporated into the amplifying viral DNA, causing chain termination and preferentially disrupting either viral transmission or viral replication while minimizing the effects on the host (Johnston and Corey, 2016). Although antiviral medications can reduce the severity and frequency of symptoms, they still cannot completely eliminate the virus. In addition to antiviral medications, antibody drugs and vaccines are also effective measures to control HSV infection. Antiviral monoclonal antibodies (mAbs) are promising therapeutics against HSV. To date, a few mAbs, such as D4.2 (Lathey et al., 1986), Hu-mAb#33 (Clementi et al., 2017), III-174 (Sherwood et al., 1996), and hu2c (Krawczyk et al., 2013), have shown therapeutic efficacy against HSV infection. Nonetheless, no single antibody is currently used for the treatment of HSV infection in the clinic. MAbs targeting functional epitopes on HSV entry glycoproteins mediate HSV neutralization, neutralizing viral infectivity by blocking the interaction between HSV entry glycoproteins and their receptors or interfering with fusion-inducing glycoproteins interacting with each other (Atanasiu et al., 2021; Cairns et al., 2014a, 2020). Most mAbs that have virus-neutralizing activity and recognize discontinuous epitopes may have low virus-neutralizing ability, while those mAbs recognizing continuous epitopes may have high virus-neutralizing ability (Cairns et al., 2014b; Du et al., 2017). Thus, the identification of new functional epitopes for NAbS would facilitate the development of therapeutic antibody drugs or vaccine design. Furthermore, because HSV infections are incurable once they occur, the development of prevention strategies is particularly important. However, frustratingly, no vaccines for HSV have yet been developed and proven to be effective in clinical trials (Belshe et al., 2012; Corey et al., 1999; Johnston et al., 2011; Koelle and Corey, 2003, 2008). Therefore, there is an urgent need to develop novel prevention strategies for HSV infection.

In this study, we found several mAbs with cross-neutralizing activity against HSV-1 and HSV-2. 4A3 showed the highest neutralizing activity among them, inhibiting viral cell-to-cell transmission and interfering with the viral attachment step between HSV and host cells. In addition, 4A3 could protect BALB/c mice from lethal HSV-2 challenge. Furthermore, we showed that 4A3 recognized a highly conserved continuous epitope (residues 216 to 220) within the receptor-binding domain of gD. The discovery of 4A3 revealed a protective epitope on HSV gD and provided guidance for rational vaccine design and the development of robust protective or therapeutic interventions.

2. Materials and methods

2.1. Cell lines and viruses

U-2 OS, Vero, 293T, HEL299, HFF-1, HeLa and B16-F10 cells (which express neither nectin-1 nor HVEM (Miller et al., 2001)) were obtained from American Type Culture Collection (ATCC). L-O2 cells were obtained from the China Infrastructure of Cell Line Resources. Primary human umbilical vein endothelial cells (HUVECs) were purchased from ScienCell and cultured according to the manufacturer's instructions (ScienCell). All cell lines were tested for mycoplasma and cultured in Dulbecco's modified Eagle medium (DMEM) supplemented with 10% fetal bovine serum (FBS) and antibiotics at 37 °C and with 5% CO₂. HSV-1 (KOS strain) and HSV-2 (G strain) were purchased from ATCC, propagated and titrated in U-2 OS cells, and stored at -80 °C.

2.2. Plasmids and transfection

Lenti-puro was purchased from Addgene. The gene encoding HSV-1 gD (gD1) or HSV-2 gD (gD2) was amplified from the KOS genome or G genome and cloned into the pLenti-puro vector to obtain pLenti-gD1 or pLenti-gD2, respectively. The genes encoding gD mutants, gB, gL, and

Nectin-1 were commercially synthesized (GENEWIZ) and inserted into the pLenti-puro vector. The gene encoding the gD1 ectodomain (Lys 1-Met 316) with a 6 × His tag at the C-terminus was commercially synthesized (GENEWIZ) and inserted into the pTT5 vector (CNRC) to obtain pTT5-gD1-His. All plasmids were transfected into 293T cells using Lipofectamine 2000 (Invitrogen) according to the manufacturer's instructions. Recombinant gD1-His protein was purified from pTT5-gD1-His-transfected cell supernatant by using Ni-NTA chromatography (GE Healthcare) according to the manufacturer's instructions. The gD1-His protein was eluted using 100 mM imidazole and dialyzed in PBS.

2.3. ELISPOT-based neutralization test (ELISPOT-NT)

U-2 OS cells were seeded in 96-well plates at a density of 10⁴ cells per well and incubated for 24 h until the cells formed a monolayer. Antibodies were diluted to 2 µg/ml, and followed by continuous twofold gradient dilution. A total of 10⁴ PFU of viruses in a volume of 60 µl were mixed with an equal volume of serially diluted antibody and incubated at 37 °C for 1 h in 96-well U bottom plates. Then, the mixture was added to the monolayer cells and incubated for 14 h. The supernatants were discarded, and the cells were fixed with 1% paraformaldehyde in the dark at room temperature for 5 min. The cell plates were washed 3 times with PBS. A primary anti-HSV-1 gD antibody (Santa Cruz) was added to the cell plates, and the plates were incubated at 37 °C for 1 h. Then, a goat anti-mouse IgG HRP-conjugated secondary antibody (Invitrogen) was added to the cell plates, and the plates were incubated at 37 °C for another 1 h. After washing with PBS, chromogenic solutions A and B (Beyotime) were mixed in equal proportions and added to the cell plates. The number of spots in the cell plates was read by an ImmunSpot@S5 UV Analyzer (Cellular Technology Limited). The raw data of each sample obtained by the enzyme-linked immunospot assay (ELISPOT)-based neutralization test (ELISPOT-NT) method were calculated with the following formula according to a previously reported protocol: Inhibition ratio (%) = 100 × ((average spot counts for virus control - average spot counts for each concentration)/average spot counts for virus control) (Luo et al., 2016). The neutralizing antibody activity can be interpreted as the highest antibody concentration that neutralized 50% of the virus (IC₅₀), which was calculated by nonlinear, dose-response regression analysis using GraphPad Prism software ("log (agonist) vs response – Variable Slope (four parameters)" function).

2.4. Generation of mAbs

For preparation of mAbs against HSV, six-week-old female BALB/c mice were immunized with a mixture of HSV KOS and G strains in equal proportions by standard vaccination procedures. Briefly, mAbs were raised in mice using an intraperitoneal injection of 10⁶ PFU equivalents of UV-inactivated HSV-1/2 emulsified in Freund's complete adjuvant, followed by a booster injection in the superficial gluteal muscle one month later. Hybridoma cells were obtained at two months post-immunization as previously reported (Huang et al., 2012). The supernatants of hybridoma cells were screened by the cell-based ELISPOT method and ELISPOT-NT method. The positive clones were selected by their neutralizing activities against both HSV-1 and HSV-2. Mabs were prepared by ascites production and purified by using protein G chromatography (GE Healthcare) according to the manufacturer's instructions.

2.5. Plaque reduction neutralization test (PRNT)

Vero cells were seeded in 6 cm dishes at a density of 10⁶ cells per well and cultured for 2 days until the cells formed a monolayer. The 4A3 and 8H2 antibodies were diluted at 1 µg/ml, 0.5 µg/ml, 0.25 µg/ml, 0.125 µg/ml, 0.063 µg/ml and 0.032 µg/ml. Each antibody dilution was repeated in triplicate. One hundred PFU of virus were incubated with antibodies at 37 °C for 1 h and then added to Vero cells. After another 2 h

of incubation at 37 °C, the cell monolayers were overlaid with 10 ml of 2% methylcellulose medium containing antibodies and then incubated at 37 °C for 72 h. Finally, the cells were stained with 5 ml of 0.01% neutral red overnight, and then, the plaques were manually counted using a white light transilluminator. The 50% inhibitory concentration (IC_{50}) of each sample was defined as the highest antibody concentration that caused a 50% plaque reduction.

2.6. Western blotting

Western blotting was performed as previously described (Geng et al., 2012). In brief, virus-infected cells were lysed in RIPA lysis buffer containing protease inhibitor cocktail. Cell lysates were separated by SDS-PAGE and transferred onto a nitrocellulose membrane. After the membranes were blocked with 5% BSA for 1 h, they were probed with the indicated primary antibodies overnight at 4 °C, incubated with the HRP-conjugated secondary antibodies for 1 h at room temperature, and finally visualized with Lumi-Light^{PLUS} Western Blotting Substrate (Roche). An anti-gD antibody (DL6) that recognizes the denatured gD was obtained from Santa Cruz.

2.7. Dot blot analysis

U-2 OS cells transfected with pLenti-puro-gD1 or pLenti-puro-gD2 were lysed with lysis buffer without denaturing agents (20 mM HEPES, 1 mM EGTA, 5 mM MgCl₂, 100 mM NaCl, 4 mg/ml Decyl-β-D-maltopyranoside, 10% glycerol and protease inhibitor cocktail). Cell lysates were directly dot printed onto a nitrocellulose membrane using a Bio-DOT instrument (Bio-Rad). The subsequent steps were performed as previously described for western blotting.

2.8. Immunofluorescence assay (IFA)

In brief, cells on glass slides were fixed with 1% paraformaldehyde and permeabilized with 0.1% Triton X-100. After blocking with 5% goat serum in PBS for 1 h, the slides were stained with the indicated antibodies overnight at 4 °C, and then incubated with FITC-conjugated secondary antibody before examination using a confocal microscope.

2.9. Cell-to-cell spread assay

The cell-to-cell spread assay was based on a previously described protocol (Krawczyk et al., 2011). Monolayer Vero cells were first infected with viruses at an MOI of 0.01, and the viruses were removed at 4 h post-infection. The cells were washed with PBS 3 times and then incubated in DMEM containing 2% FBS in the presence of the antibodies 4A3 (50 µg/ml) and 8H2 (50 µg/ml). An irrelevant antibody was used as a negative control. Then, 48 h later, the cells were subjected to an immunofluorescence assay (IFA).

2.10. Preattachment or postattachment neutralization assay

The preattachment or postattachment neutralization assays were performed as previously described (Krawczyk et al., 2011). In brief, a virus-antibody mixture was incubated for 1 h at 4 °C before inoculation over monolayer Vero cells (preattachment). Monolayer Vero cells were prechilled (4 °C for 15 min) and infected with viruses at 4 °C for 1 h before serial dilutions of antibodies were added to the monolayer (postattachment). Then, the above treated Vero cells were incubated for 2 h at 37 °C. Viral titers were assessed at 72 h post-infection using a standard plaque assay.

2.11. Animal study

The mouse intravaginal HSV-2 challenge model was established as previously described (Cena-Diez et al., 2016). To improve the

susceptibility of mice to HSV-2, six-week-old female BALB/c mice were first stimulated with medroxyprogesterone acetate (2.5 mg/mouse) before vaginal challenge with HSV-2 (Parr et al., 1994). Then, the mice were randomly divided into five groups with six or seven mice in each group, inoculated intravaginally with 10⁵ PFU HSV-2 in a volume of 20 µl and maintained in a supine position for 15 min. At 24 h post-vaginal challenge, the mice were treated daily with different doses of the 4A3 antibody by intraperitoneal injection for three consecutive days. Mice in each group were examined daily for symptoms of genital disease, body weight, and mortality. Disease score was graded on a scale of 0–4 by assigning 1 point each for erythema, exudate, hair loss, and paralysis (Awasthi et al., 2012; Du et al., 2017).

2.12. Hematoxylin and eosin (H&E) staining

Brain and vaginal tissues of mice were fixed in 10% formalin, embedded in paraffin, and stained with hematoxylin and eosin (H&E) according to previously described methods (Luo et al., 2020). Then, the sections were washed and mounted with cover slips. Images were captured with a research-level upright microscope (Olympus).

2.13. Flow cytometry

10⁶ B16-F10 cells stably expressing Nectin-1 were coincubated with a mixture of serially diluted 4A3 and 10⁶ PFU of virus at 37 °C for 12 h. After washing twice with PBS, the cells were stained with FITC-conjugated anti-gD secondary antibody at 4 °C for 30 min in the dark. After washed twice with PBS, the number of FITC-positive cells was determined by flow cytometry (BD Bioscience LSRIFortessa X-20). The inhibition ratio (%) = 100 × ((average FITC-positive cells for virus control - average FITC-positive cells for each concentration)/average FITC-positive cells for virus control).

293T cells transfected with pLenti-puro-gD1 (gD WT) were coincubated with a mixture of serially diluted 4A3 and 0.5 µg/ml His-tagged Nectin-1 (Sino Biological) or 1 µg/ml His-tagged HVEM (Sino Biological) at 4 °C for 1 h. After washing twice with PBS, the cells were stained with FITC-conjugated anti-His secondary antibody at 4 °C for 30 min in the dark. After washed twice with PBS, the number of FITC-positive cells was determined by flow cytometry.

293T cells transfected with plasmids expressing individual gD mutants were incubated with 10 µg/ml 4A3 at 4 °C for 30 min and washed twice with PBS. Then, the cells were stained with PE-conjugated goat anti-mouse IgG antibody at 4 °C for 30 min. After washed twice with PBS, the number of positive cells was determined by flow cytometry. 293T cells stained with an irrelevant antibody were used as negative controls, and 293T cells transfected with gD WT were used as positive controls.

2.14. Chemiluminescence immunoassay (CLIA)

The binding ability of gD and Nectin-1 (Sino Biological) was determined by an indirect chemiluminescence immunoassay (CLIA). Briefly, 96-well plates were coated with 50 ng/well Nectin-1-Fc protein (Sino Biological), and nonspecific binding was blocked with PBS containing 5% BSA. Serially diluted gD-His protein was added to the wells for a 1 h of incubation, followed by washing and reaction with HRP-conjugated anti-His antibody (Proteintech) for 30 min at 37 °C. After addition of the luminol substrate (Wantai BioPharm) for 5 min, the plates were examined with a chemiluminescence reader (Berthod).

The ability of 4A3 to block the interaction between Nectin-1 and gD was evaluated by a competitive CLIA. Serially diluted 4A3 or a mouse IgG1 isotype control (R&D Systems) and gD-His proteins (1 µg/ml) were added to the Nectin-1-precoated plate and incubated for 1 h at 37 °C. Then, HRP-conjugated anti-His antibody (Proteintech) was added to the wells for 30 min of incubation, followed by washing, reaction and detection.

2.15. Statistical analyses

Statistical analyses were performed using GraphPad Prism software (GraphPad Software). The data are presented as the mean \pm standard deviation (SD). Statistical parameters and methods are reported in the Figure Legends. Data for survival were analyzed by the log-rank (Mantel-Cox) test. P values were calculated, and differences were reported as significant using *($p < 0.05$), ** ($p < 0.01$), or *** ($p < 0.001$).

3. Results

3.1. Generation of neutralizing mAbs against HSV

To obtain mAbs with cross-neutralizing activity against both HSV-1 and HSV-2, we immunized BALB/c mice with HSV-1 and HSV-2 in equal proportions. A total of 14 antibodies with good reactivity against HSV were obtained (Figs. S1A and S1B), and only five of them had virus-neutralizing activity, namely, 4A3, 8H2, 5F11, 2F5 and 2B8 (Figs. S1C and S1D). The neutralizing activity of the five antibodies against HSV was further evaluated by ELISPOT-NT, as shown in Fig. 1A and Fig. 1B, which showed that the five antibodies all had neutralizing activity against the two types of HSV. Furthermore, by calculating the 50% virus-inhibitory concentrations (IC_{50}) of these antibodies against HSV, we found that 4A3 and 8H2 had high neutralizing activity against HSV-1 and HSV-2 ($IC_{50} < 200$ ng/ml) (Fig. 1C and D), while 5F11, 2F5 and 2B8 had relatively low neutralizing activity against HSV-2 ($IC_{50} > 250$ ng/ml) (Fig. 1D).

To further evaluate the neutralizing activity of 4A3 and 8H2 against HSV, a viral plaque reduction neutralization test (PRNT) was performed. The PRNT results demonstrated that 4A3 and 8H2 neutralized HSV-1 and HSV-2 in a dose-dependent manner; as the concentration increased to 0.1 μ g/ml, HSV-1 and HSV-2 infection was completely abolished (Fig. 2A and B). 4A3 and 8H2 had similar potency against

HSV-1; however, 4A3 exhibited higher potency against HSV-2, with an IC_{50} of 59.88 ng/ml (Fig. 2C and D). We also evaluated the neutralizing activity of 4A3 and 8H2 in B16-F10 mouse melanoma cells expressing Nectin-1. It was observed that 4A3 also had higher neutralizing activity against HSV-2 compared with 8H2 (Fig. 2E and F). These data suggested that the neutralizing activity of 4A3 against HSV-1 and HSV-2 was higher than that of 8H2. Therefore, 4A3, having a high cross-neutralizing activity against HSV, was chosen for further characterization.

3.2. 4A3 blocks cellular infection and cell-to-cell spread of HSV

To further evaluate the neutralizing effects of 4A3 against HSV-1 and HSV-2, we tested the ability of 4A3 to block viral infection in normal human cells, including L-O2 (a normal liver cell line), HFF-1 (human skin fibroblast cells), HUVECs (human umbilical vein endothelial cells) and HEL299 (human lung fibroblast cells). These cells were infected with HSV at an MOI of 1, and the remaining viable cells were counted by trypan blue staining at 72 h post-infection. As shown in Fig. 3A-D, both HSV-1 and HSV-2 had a strong cell-killing ability in these cells, suggesting that various types of cells were susceptible to HSV-1 and HSV-2 infection. The neutralizing activity of 4A3 against HSV was further assessed in these cells. The cell-killing ability of HSV-1 and HSV-2 was significantly inhibited by 4A3, and almost all cells survived after 4A3 treatment. Furthermore, Western blot analysis showed that the expression of gD was undetectable at 6, 12 or 24 h after HSV infection when the cells were treated with 4A3 (Fig. 3E and F), indicating that virus infection in these cells was completely blocked by 4A3. The above results proved that 4A3 protected human cells from HSV-1 and HSV-2 infection.

In the process of viral infection, bridging fibers can be formed between adjacent cells through filopodia, and viruses can spread from infected cells to uninfected cells through the bridging fibers to evade

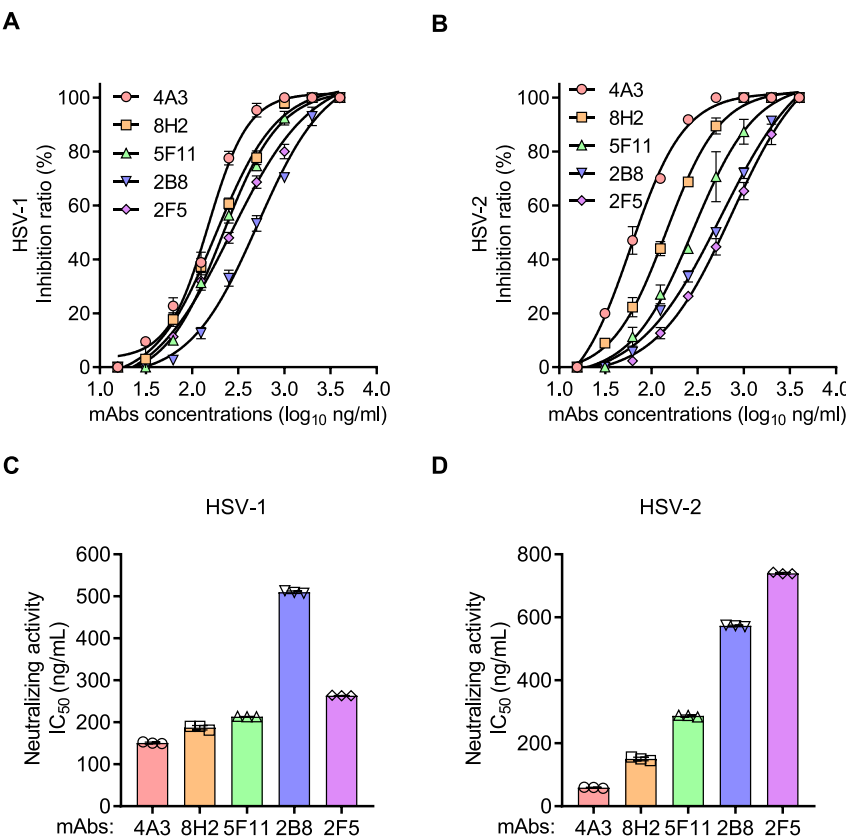


Fig. 1. Generation of mAbs against HSV. (A) The neutralizing effect of five antibodies against HSV-1 was evaluated by ELISPOT-NT. HSV-1 or HSV-2 was incubated with serially diluted antibodies at 37 °C for 1 h and then used to infect U-2 OS cells. The neutralizing activities of mAbs were detected by ELISPOT-NT at 14 h post-infection. The inhibition ratio was calculated relative to the negative control. (B) The neutralizing effect of five antibodies against HSV-2 was evaluated by ELISPOT-NT. (C) and (D) The 50% virus-inhibitory concentrations (IC_{50}) of these antibodies against HSV was calculated. All the data are presented as the mean \pm SD from at least three independent experiments.

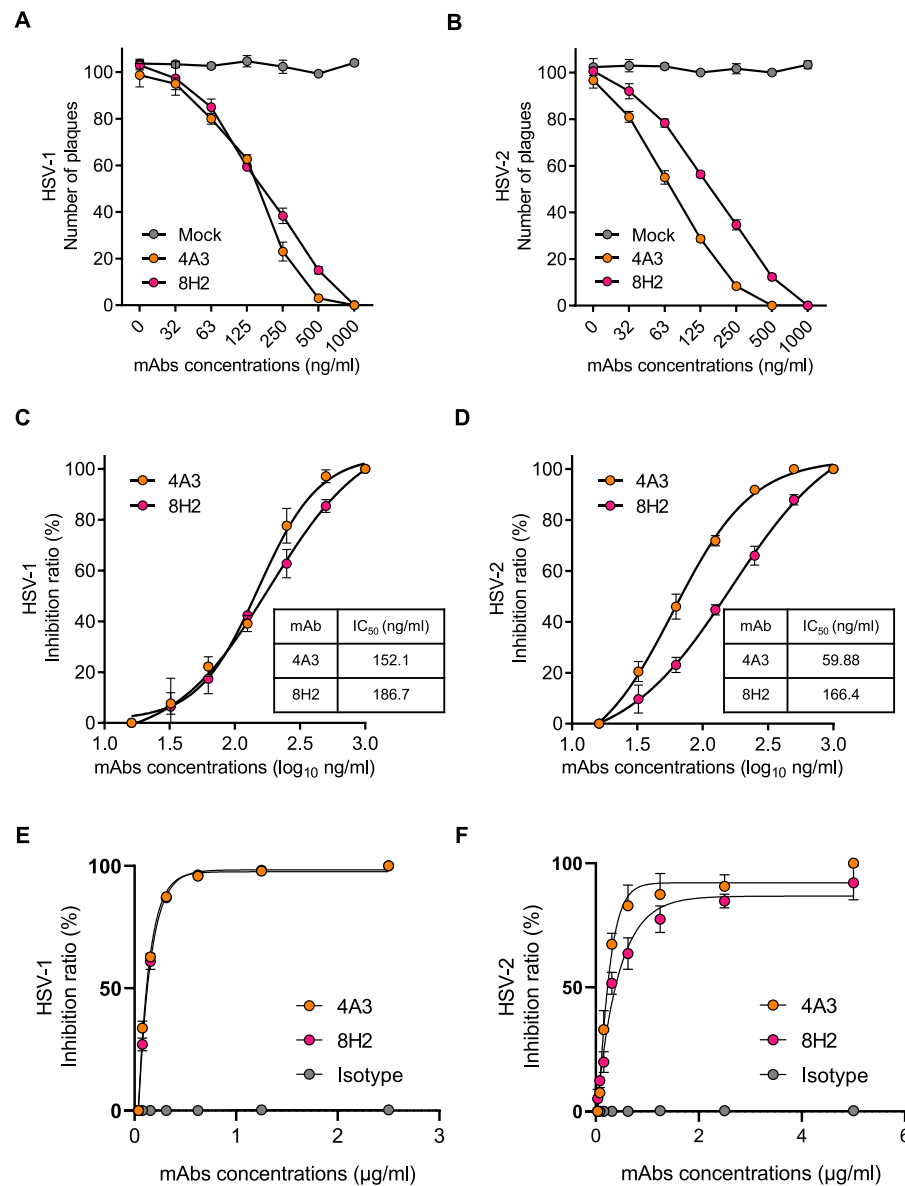


Fig. 2. Evaluation and comparison of the neutralizing effects of 4A3 and 8H2. (A) The neutralizing effects of 4A3 and 8H2 against HSV-1 were evaluated by PRNT. (B) The neutralizing effects of 4A3 and 8H2 against HSV-2 were evaluated by PRNT. (C) and (D) The 50% virus-inhibitory concentrations (IC₅₀) of 4A3 and 8H2 against HSV were calculated. (E) The neutralizing effects of 4A3 and 8H2 against HSV-1 were evaluated in B16-F10 mouse melanoma cells expressing either Nectin-1. (F) The neutralizing effects of 4A3 and 8H2 against HSV-2 were evaluated in B16-F10 mouse melanoma cells expressing Nectin-1. All the data are presented as the mean \pm SD from at least three independent experiments.

immune surveillance. Blocking cell-to-cell spread is considered to be an important aspect for evaluating the protective efficacy of Nabs. Therefore, we analyzed the ability of 4A3 to inhibit the cell-to-cell spread of HSV using IFA. The results revealed that HSV could not spread through Vero cells, and the cell-to-cell spread of HSV was blocked when Vero cells were treated with 4A3. In contrast, HSV spreads rapidly between cells by forming viral plaques (Fig. 3G and H). The results clearly suggested that 4A3 can inhibit cell-to-cell transmission effectively in HSV-infected cells.

3.3. 4A3 neutralizes HSV-1 and HSV-2 infection at the prebinding stage

To further explore the neutralizing mechanism of 4A3, we compared the neutralizing efficacy of 4A3 when antibodies were added before (preattachment) or after (postattachment) HSV virions interacted with Vero cells. 8H2 was chosen as a control. Enhanced inhibition of HSV infection was observed as the concentration of 4A3 or 8H2 increased. When 4A3 was added before virus-host interaction (preattachment), approximately 85% inhibition of HSV-1 infection was observed at a concentration of 1 μg/ml (Fig. 4A), and when 4A3 was added after HSV-1 virions interacted with Vero cells (postattachment), approximately

65% inhibition of HSV-1 infection was observed at a concentration of 1 μg/ml (Fig. 4B). The neutralizing efficacy of 4A3 against HSV-1 was better in the preattachment treatment than in the postattachment treatment. The neutralizing efficacy of 4A3 against HSV-2 was quite different when the antibody was added before the HSV-2 virions interacted with Vero cells compared to that observed upon treatment after the interaction. Approximately 97% inhibition of HSV-2 infection was observed in the preattachment treatment (Fig. 4C), and only approximately 62% inhibition of HSV-2 infection was observed in the postattachment treatment, with a 4A3 concentration of 1 μg/ml (Fig. 4D). Although the neutralizing efficacy of 8H2 showed a similar trend in the preattachment and postattachment assays, compared with 4A3, 8H2 had obviously weaker neutralizing ability against HSV-2 both before and after the virions were incubated with cells. The neutralizing efficacy of 4A3 on HSV infection was better in the preattachment treatment than in the postattachment treatment, indicating that 4A3 interfered with the virus binding process and neutralized HSV entry at the prebinding stage. Moreover, 4A3 could still neutralize HSV after virus attachment, suggesting that the affinity between 4A3 and the HSV entry protein may be higher than that between the HSV entry protein and its cell receptor.

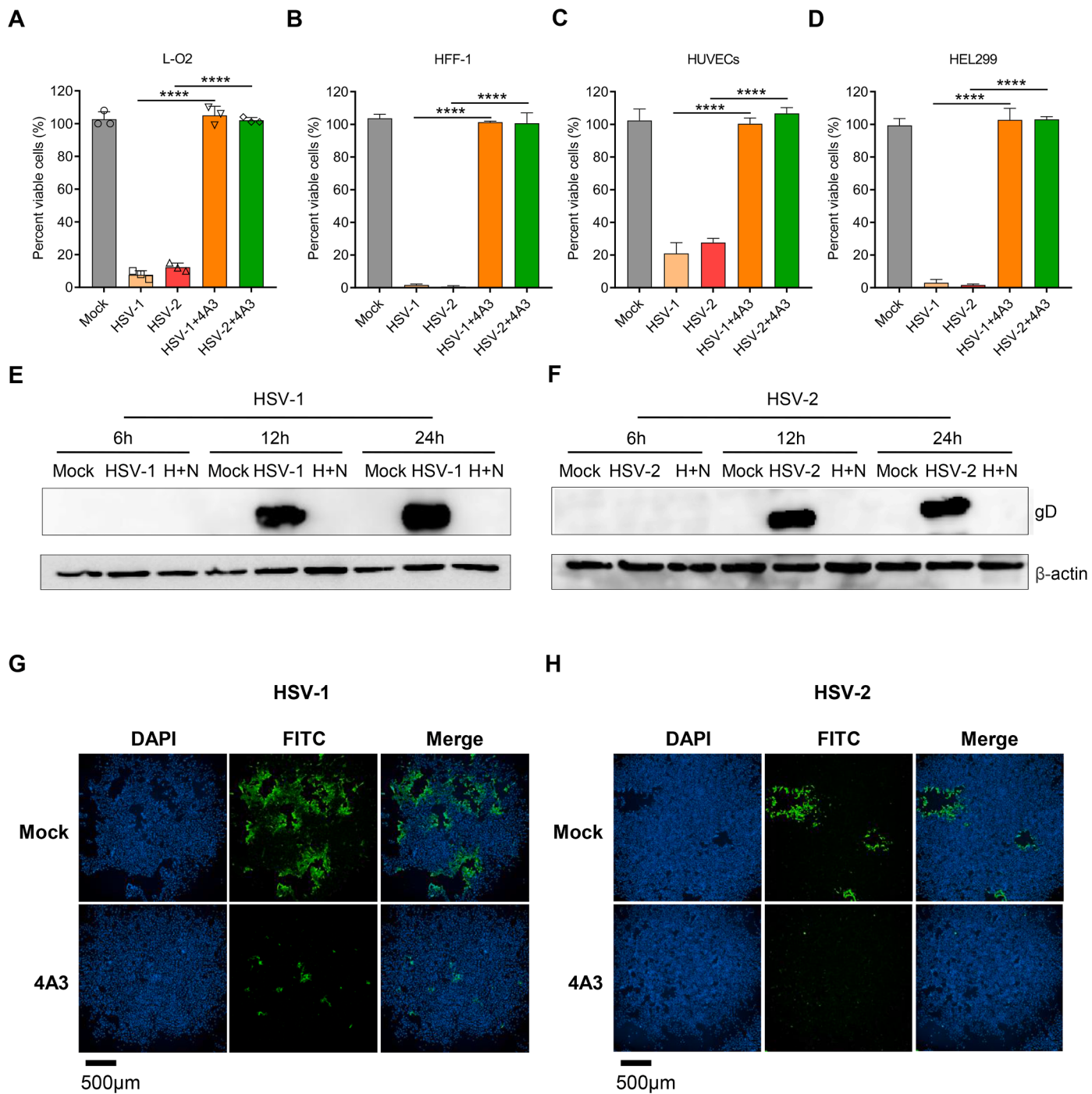


Fig. 3. 4A3 blocks cellular infection and cell-to-cell spread of HSV-1 and HSV-2. (A) L-O2 cells, (B) HFF-1 cells, (C) HUVECs and (D) HEL229 cells were infected with HSV-1 and HSV-2 at an MOI of 1, and cell monolayers were treated with an excess of 4A3 antibody (10 µg/ml). Irrelevant mouse IgG (10 µg/ml) or culture medium (mock) alone was used as a control. Viable cells were counted by trypan blue staining at 72 h post-infection. (E and F) Virus-infected HFF-1 cells were treated with 4A3 antibody (10 µg/ml) or culture medium (mock) and then harvested for Western blot analysis using gD antibody as the primary antibody at 6 h, 12 h and 24 h post-infection. (G and H) Cell-to-cell spread of HSV-1 and HSV-2 in Vero cells was detected by IFA. Vero cells were infected with HSV-1 and HSV-2 at an MOI of 0.01, and then 4A3 was added at 4 h post-infection. Cells were fixed and observed by fluorescence microscopy at 48 h post-infection. The uninfected cells were used as the mock control. All the data are presented as the mean ± SD from at least three independent experiments. Significant differences were analyzed by unpaired two-tailed Student's *t*-test (A–D).

3.4. 4A3 protects mice from lethal HSV-2 infection

To evaluate the protective efficacy of 4A3 *in vivo*, we established a female BALB/c mouse model with lethal HSV-2 challenge. We used medroxyprogesterone acetate to pretreat the mice before HSV-2 infection, and then, the mice were vaginally infected with a lethal dose of

HSV-2 viruses. The mice were treated intraperitoneally with 0, 1, 5, 10, or 20 mg/kg 4A3 at 24 h after intravaginal HSV-2 challenge, and then repeatedly received the same treatment regimen on day 1 and 2 after the initial treatment (Fig. 5A). In the PBS-treated group and low-dose treatment group (1 mg/kg), HSV-2 challenge resulted in rapid progressive disease (Fig. 5B), and a series of abnormal symptoms appeared,

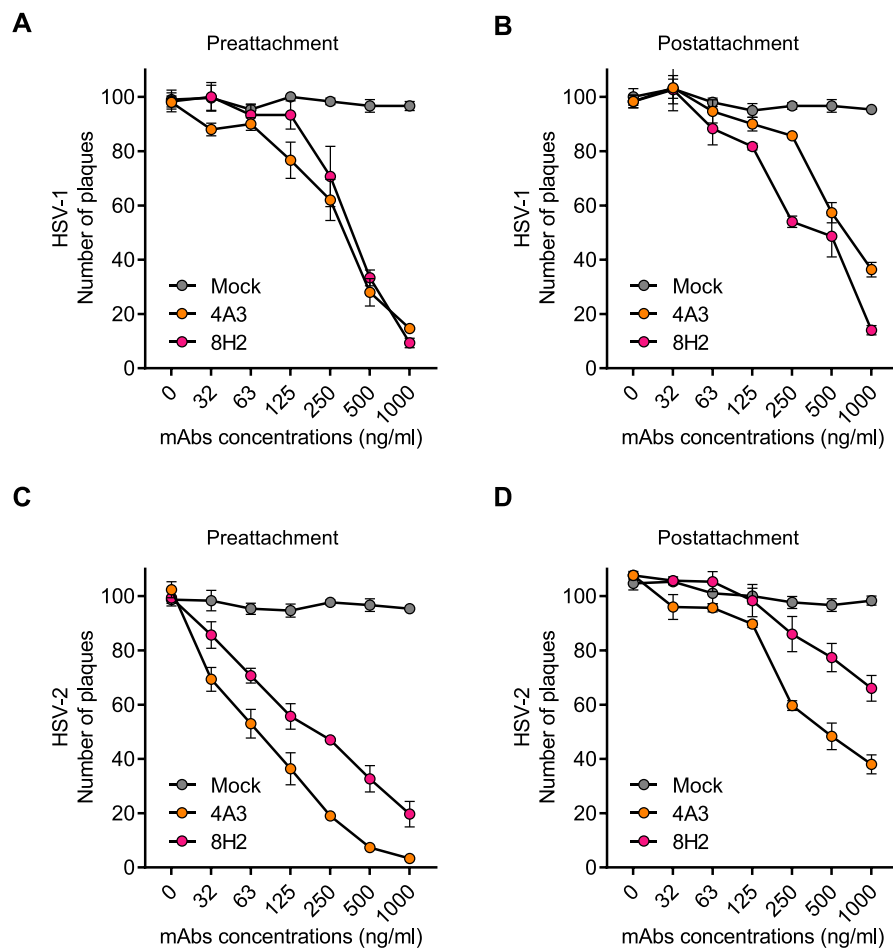


Fig. 4. Mechanism of 4A3-mediated neutralization. Comparison of the neutralization efficacy of 4A3 when serial dilutions of the antibody were added before (A and C, preattachment) or after (B and D, postattachment) HSV virions interacted with Vero cells. 8H2 was used as a control. Neutralization effects were determined after 72 h post-infection by the standard plaque assay. All the data are presented as the mean ± SD from at least three independent experiments.

such as significant body weight loss (Fig. 5C), genital lesion and behavioral disorder; these mice began to die at 5 days post-infection (Fig. 5D). In contrast, no symptoms or body weight loss were observed in the medium-dose treatment group (5 mg/kg and 10 mg/kg) and high-dose treatment group (20 mg/kg), and all the mice survived in these groups.

To further explore the influence of HSV-2 infection on vital tissues and organs of BALB/c mice, the brain and vaginal tissues of the mice were harvested at 7 days post-infection and subjected to H&E staining. Obvious pathological damage in the brain and vaginal tissues was observed in the PBS-treated group. However, 4A3 completely blocked the infection of HSV-2 in the brain and vaginal tissues of mice and protected the mice from damage caused by a lethal dose of HSV-2 (Fig. 5E). These animal study results indicated that 4A3 had significant protective effects against HSV-2 genital infection *in vivo* in a dose-dependent manner.

3.5. Characterization of 4A3

We first analyzed the antibody subclass of 4A3 using ELISPOT and showed that 4A3 was an IgG1-type mAb (Fig. 6A). Furthermore, to characterize the specific HSV entry protein recognized by 4A3, we evaluated its ability to recognize denatured and native forms of HSV gD by Western blot and dot blot analyses. The Western blot results demonstrated that 4A3 could not bind to HSV gD in the presence of denaturing agents (Fig. 6B). In contrast, 4A3 could bind specifically to

HSV gD in the absence of denaturing agents (Fig. 6C), indicating that the recognition of the epitope on gD by 4A3 was based on conformation. The IFA results also showed that 4A3 could specifically bind to naïve forms of gD in Vero cells infected with HSV-1 or HSV-2 (Fig. 6D). These results indicated that 4A3 could specifically recognize the native forms of the HSV gD protein.

3.6. 4A3 interferes with gD binding to its cellular receptor Nectin-1

To date, four cellular receptors for HSV gD have been identified, including Nectin-1, Nectin-2, HVEM and 3-O-HS. Nectin-1 and HVEM can bind to two types of HSV-1, Nectin-2 is a weak receptor of HSV-2, and 3-O-HS binds only to HSV-1 (Campadelli-Fiume et al., 2000). Because 4A3 can recognize HSV gD and interfere with the virus binding process at the prebinding stage, we speculated that 4A3 may occupy the Nectin-1- or HVEM-binding epitope on gD and then block the binding of virions to Nectin-1 or HVEM. To verify this hypothesis, we used gD-overexpressing 293T cells to study the binding activity between naïve gD expressed on the surface of 293T cells and recombinant Nectin-1 or HVEM protein. Flow cytometry analysis revealed that both the Nectin-1 and HVEM proteins could specifically bind to gD when 4A3 was not added (Fig. 7A). The addition of 4A3 significantly inhibited the binding of Nectin-1 to gD in a dose-dependent manner, and the binding of Nectin-1 to gD was almost completely inhibited when the concentration of 4A3 reached 100 µg/ml (Fig. 7B). However, the addition of 4A3 had no significant effect on the binding of HVEM to gD (Fig. 7C).

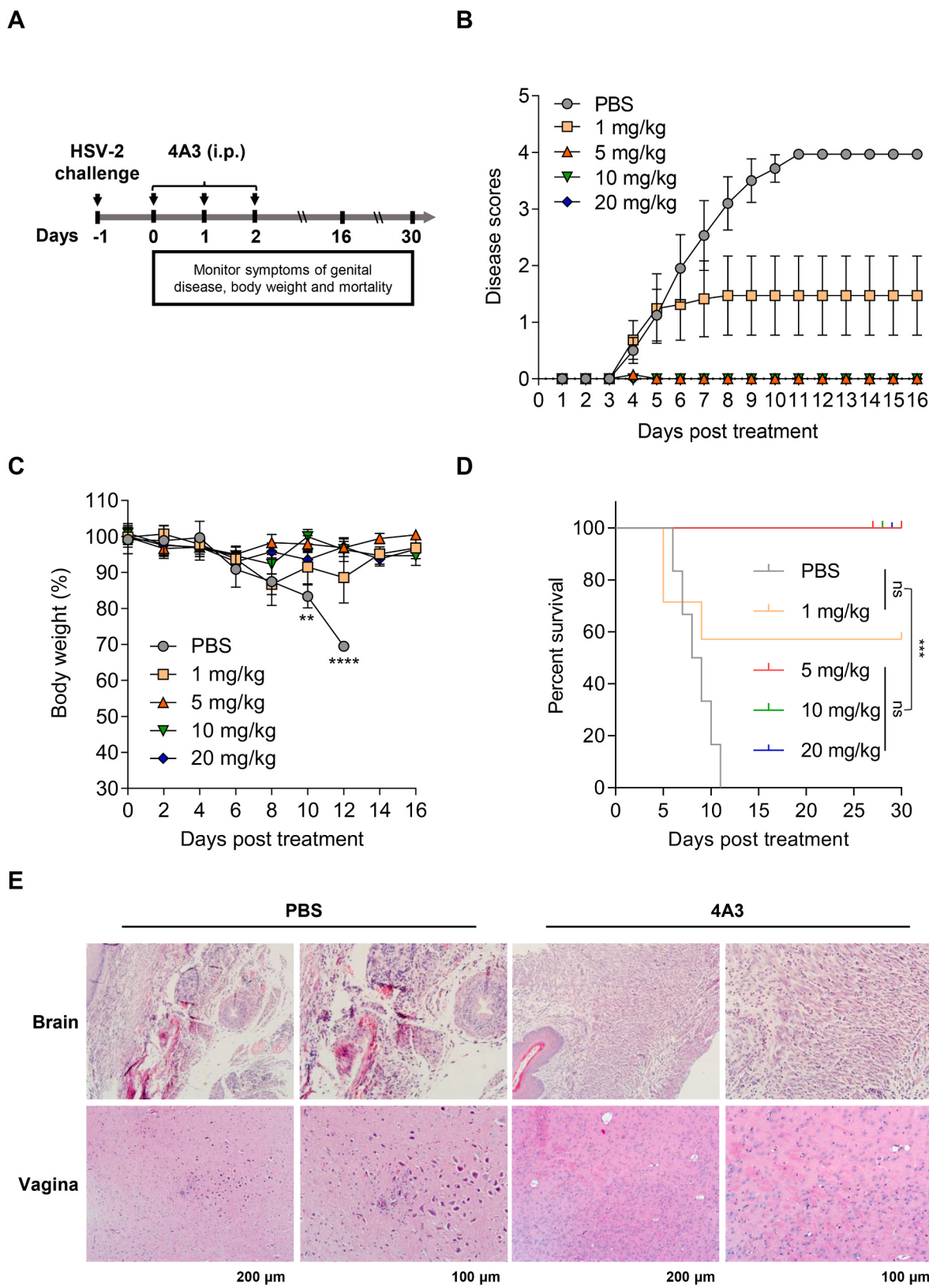


Fig. 5. 4A3 protects mice from lethal HSV-2 infection. Mice were challenged with a lethal dose of HSV-2 through the vagina. The treatment group was treated with various doses of 4A3, while the control group was treated with PBS. (A) Schematic diagram of the treatment regimen. (B) Symptoms of genital disease in each group was scored daily over a 16-day period after 4A3 treatment. (C) The body weight of mice was recorded every two days over a 16-day period and was expressed as a percentage of the value prior to treatment. (D) The survival of mice in each group was monitored over a 30-day period. (E) The vaginal and brain tissues of the treatment group receiving 5 mg/kg 4A3 or the control group were examined by H&E staining. The data represent results from one of three independent experiments with $n = 6$ or 7 per group. Significant differences were analyzed by unpaired two-tailed Student's *t*-test (C) and Log-rank (Mantel-Cox) test (D).

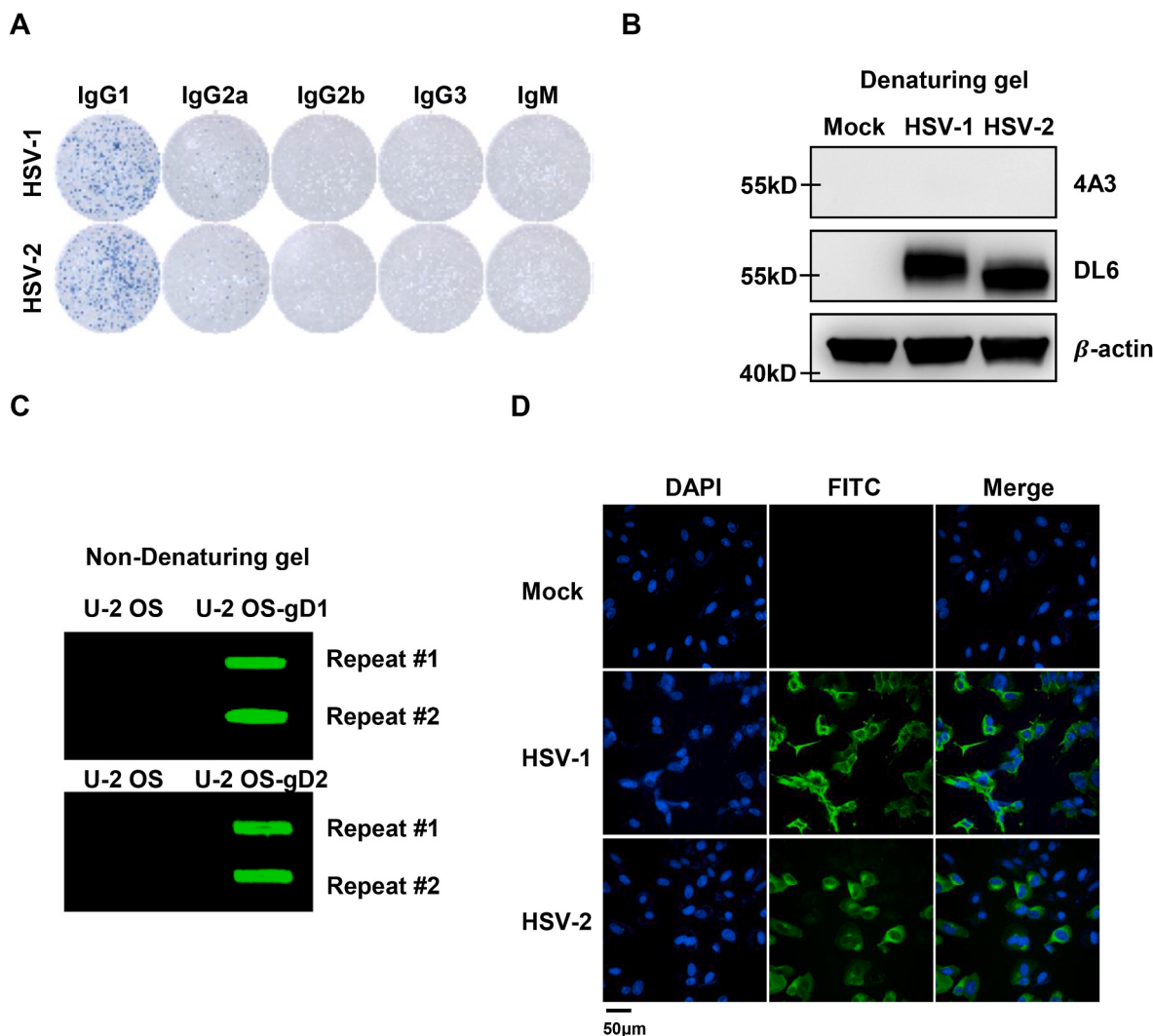


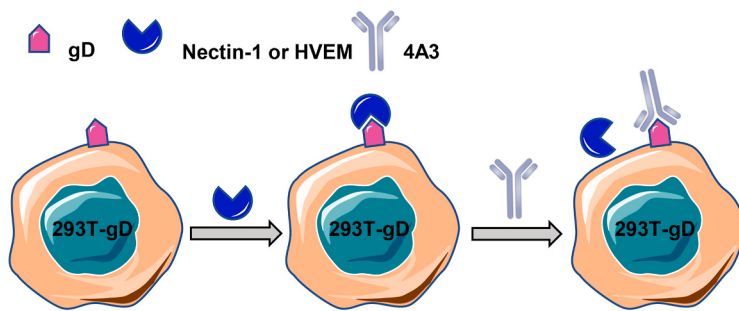
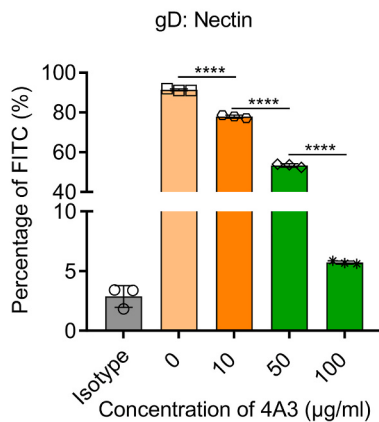
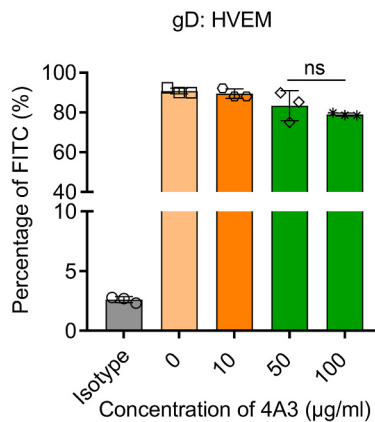
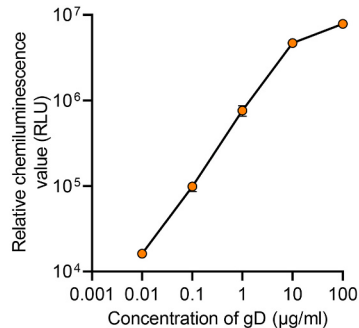
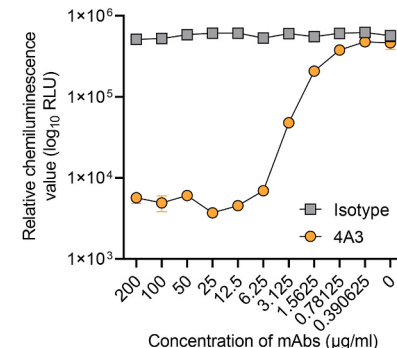
Fig. 6. Characterization of 4A3. (A) The antibody subtype of 4A3 was determined using ELISPOT. (B) Western blot analysis of the reactivity between denatured gD and 4A3. Vero cells were infected with HSV-1 and HSV-2 at an MOI of 1, cell lysates were collected using RIPA lysis buffer containing denaturing agents at 24 h post-infection, and 4A3 or DL6 was used as the primary antibody. (C) Dot blot analysis of the reactivity between nondenatured gD and 4A3. Cell lysates from U-2 OS cells or gD overexpressing U-2 OS cells were collected using lysis buffer without denaturing agents. Two independent experiments are shown (repeat #1 and repeat #2). (D) The reactivity of 4A3 with HSV-1 and HSV-2 was determined by IFA. Vero cells were infected with HSV-1 and HSV-2 at an MOI of 1, cells were fixed and subjected to IFA using 4A3 as the primary antibody at 24 h post-infection, and FITC-conjugated goat anti-mouse IgG served as the secondary antibody. Infected cells staining with a mouse IgG1 isotype were used as the negative control.

Furthermore, we further verified the ability of 4A3 to block the binding of the gD ectodomain to Nectin-1 using CLIA. The results demonstrated that the gD ectodomain could bind to Nectin-1 in a dose-dependent manner (Fig. S2 and Fig. 7D). The binding of Nectin-1 to the gD ectodomain was almost completely inhibited when the concentration of 4A3 reached 3.125 µg/ml (Fig. 7E). These results suggested that 4A3 mainly interferes with gD binding to its cellular receptor by competing with the Nectin-1 binding epitope rather than the HVEM binding epitope on the gD ectodomain, thus blocking HSV entry.

3.7. Detailed epitope mapping of 4A3

Because 4A3 has cross-neutralizing activity against HSV-1 and HSV-2, we speculated that the precise epitope involved in the binding of 4A3 to gD mainly involves the conserved amino acids between HSV-1 and HSV-2 rather than different amino acids. In addition, previous results have shown the possible epitope involved in the binding of Nectin-1 to gD; the patch1 residues (P23, L25 to Q27, F223, N227, V231, and Y234) and patch2 residues (R36 to H39, Q132, R134, V214 to R222) of gD

were found to be critical for Nectin-1 binding (Connolly et al., 2005; Di Giovine et al., 2011; Lu et al., 2014). To accurately identify the epitope recognized by 4A3, we constructed a series of gD mutants in which the patch1 residues and/or patch2 residues of the HSV-1 gD protein were replaced with alanine (Table 1 and Fig. 8A). Flow cytometry results showed that 4A3 bound well to gD WT but did not bind to the gD mutants when the patch1 and patch2 residues were mutated simultaneously or only the patch2 residues were mutated. This result indicated that the key epitope involved in the binding of 4A3 to gD was located in the patch2 residues. Furthermore, by reducing the number of mutated amino acids in the patch2 residues, we found that 4A3 showed very weak binding to a gD mutant (patch 2, S216 to L220), in which all the residues in the amino acid sequence from S216 to L220 were mutated simultaneously. We also investigated the effect of the individual mutation in the residues S216 to L220 on gD binding to 4A3, we found that 4A3 showed very weak binding to gD mutant (G218A) and weak binding to gD mutant (M219A), suggesting the mutation of gD residue G218 and M219 may influence the binding ability of 4A3 to gD (Fig. 8B and C). Sequence alignment showed that these residues were highly conserved

A**B****C****D****E**

between HSV-1 and HSV-2 (Fig. 8D). These results demonstrated that the whole amino acid sequence from S216 to L220 of gD was a critical part of the key epitope for 4A3 binding, and two critical residues, G218 and M219, may play the most important roles in the binding between gD and 4A3.

4. Discussion

The entry of HSV into cells is a complex and multistep process that can be divided into two glycoprotein-mediated phases, termed the viral attachment phase and viral fusion phase (Heldwein and Krummenacher, 2008). In the HSV attachment step, gB and/or gC aid virions in binding to the surface coreceptor of host cells, the heparan sulfate side chain of heparan sulfate proteoglycan (HSPG) (Shukla and Spear, 2001). Next, the HSV entry and fusion step is accomplished by the collaborative efforts of the receptor-binding protein gD, the viral fusion protein gB and the heterodimer formed by gH and gL (Turner et al., 1998). First, gD binds to one of three entry receptors, namely, HVEM, Nectin-1 and Nectin-2. The binding of the receptors and ligands prompts a

Fig. 7. 4A3 interferes with gD binding to its cellular receptor Nectin-1. (A) Schematic diagram of a competitive ligand binding assay. (B and C) Serially diluted 4A3, Nectin-1 or HVEM protein, and 293T cells stably expressing gD were coincubated at 4 °C for 1 h. The binding of Nectin-1 (B) and HVEM (C) to gD expressed on the membrane of 293T cells was measured by flow cytometry, and PBS served as a negative control. (D) The binding of serially diluted gD ectodomain to Nectin-1 (50 ng/well) was measured by CLIA. (E) The ability of 4A3 to block the interaction between Nectin-1 (50 ng/well) and gD ectodomain (1 μg/ml) was evaluated by a competitive CLIA. A mouse IgG1 isotype was used as a control. All the data are presented as the mean ± SD from at least three independent experiments.

conformational change of gD, where receptor binding displaces the C-terminus of the gD ectodomain and transmits a signal to the gH-gL heterodimer (Connolly et al., 2021). Then, gH-gL serves as a regulator of fusion that transmits a signal to gB, which activates the fusion protein gB. Finally, and most importantly, the conformational change of gB results in its insertion into the cell membrane, and then, the gB trimer refolds so that the cell and viral membranes can join together. A large number of refolded gB trimers create small holes in the cell membrane, allowing the viral capsid of HSV to enter the host cytoplasm and then be transported into the nucleus (Antoine et al., 2013; Connolly et al., 2011). In the whole viral entry process of HSV, gB, gD, gH, and gL are the most essential glycoproteins. Owing to the significant inhibitory effect on viral entry into host cells and intercellular diffusion by blocking HSV glycoproteins or their interaction with receptors, a large number of small-molecule inhibitors, vaccines, antibodies and other HSV therapeutic drugs have been designed to target HSV glycoproteins in many preclinical studies (Birkmann and Zimmermann, 2016). Furthermore, the amino acid sequence of gD is highly conserved in different HSV variants, and gD is the most common glycoprotein used in the

Table 1
gD mutants used in this study.

gD mutants	Mutation information
patch 1 and patch 2	P23A, L25A, D26A, Q27A, R36A, V37A, Y38A, H39A, Q132A, R134A, P198A, V214A, D215A, S216A, I217A, G218A, M219A, L220A, P221, R222, F223A, N227A, V231A, and Y234A
patch 1	P23A, L25A, D26A, Q27A, F223A, N227A, V231A, and Y234A
patch 2	R36A, V37A, Y38A, H39A, Q132A, R134A, P198A, V214A, D215A, S216A, I217A, G218A, M219A, L220A, P221A and R222A
Q132, P198, V214 to R222	Q132A, P198A, V214A, D215A, S216A, I217A, G218A, M219A, L220A, L220A, P221A and R222A
Q132, V214 to R222	Q132A, V214A, D215A, S216A, I217A, G218A, M219A, L220A, P221A and R222A
P198, V214 to R222	P198A, V214A, D215A, S216A, I217A, G218A, M219A, L220A, P221A and R222A
R134, V214 to R222	R134A, V214A, D215A, S216A, I217A, G218A, M219A, L220A, P221A and R222A
H39, V214 to R222	H39A, V214A, D215A, S216A, I217A, G218A, M219A, L220A, P221A and R222A
V214 to R222	V214A, D215A, S216A, I217A, G218A, M219A, L220A, P221A and R222A
D215 to P221	D215A, S216A, I217A, G218A, M219A, L220A and P221A
S216 to L220	S216A, I217A, G218A, M219A and L220A
I217 to M219	I217A, G218A and M219A
S216A	S216A
I217A	I217A
G218A	G218A
M219A	M219A
L220A	L220A

development of HSV vaccines (Bourne et al., 2003; Chowdhury et al., 2012). Therefore, the discovery of a protective conserved epitope on gD plays a positive role in the development of new HSV vaccines and therapeutic antibodies. In this study, we found that the neutralizing antibody 4A3 recognized HSV gD, and then, we explored its neutralization mechanism and identified its key binding epitope.

At present, the multiple effective NAbS for HSV mainly target the viral entry glycoprotein gD or gB. For instance, the gD-specific mAb human Ab#33 can neutralize clinical isolates of HSV at very low concentrations (Clementi et al., 2017); the gB-specific mAb hu2c can efficiently neutralize clinical isolates of HSV that are resistant to standard antiviral drugs, and the anti-HSV activity is independent of the host immunity (Krawczyk et al., 2013). In this study, five NAbS had cross-neutralizing reactivity against HSV, including gD-specific antibodies (4A3, 8H2, and 2F5), gL-specific antibodies (5F11), and gB-specific antibodies (2B8) (Fig. S3). The neutralizing activity of 4A3 and 8H2 was significantly higher than that of other three antibodies. In addition, the cross-neutralizing activity of 4A3 was better than that of 8H2 against HSV (Fig. 2). 4A3 not only had a significant neutralizing effect on HSV infection at a low concentration *in vitro* (Figs. 1 and 2) but also protected BALB/c mice effectively from lethal HSV-2 infection at a low concentration (Fig. 5). There are two possible reasons for the large difference in the neutralization abilities of different antibodies. On the one hand, different antibodies, such as 4A3 and 2B8, may bind to different viral glycoproteins; on the other hand, different antibodies, such as 4A3 and 8H2, may recognize different epitopes of viral glycoproteins. Notably, mAbs that neutralize key HSV envelope glycoproteins, such as gB and gD, are also more likely to be highly effective neutralizing antibodies.

It's intriguing that three gD NAbS (4A3, 8H2 and 2F5) in this study had different neutralizing effects against HSV. Thus, we compared the characteristics of these gD antibodies, and the findings may provide a better perspective on the benefits of 4A3. 8H2 was an IgG2a-type mAb, and 2F5 was an IgG1-type mAb (Fig. S4A). All three gD antibodies could bind specifically to HSV gD in the absence of denaturing agents, indicating that the recognition of the epitope on gD by them was based on conformation (Fig. S4B, S4C and S4D). We also investigated the key

epitope involved in the binding of 8H2 or 2F5 to gD. The results indicated that the key epitope on gD involved in the binding of 8H2 to gD was located in the patch2 residues. Compared with 4A3, more gD residues in the patch2 residues, including Q132, P198, V214, D215, S216, and L220-R222, influenced the binding of 8H2 to gD (Fig. S5A). However, the key epitope on gD involved in the binding of 2F5 to gD was mainly located outside the patch1 and patch2 residues (Fig. S5B). For 4A3, its epitopes were distinct from that seen by 8H2 and 2F5.

The risk of cell-to-cell spread-related infection of the virus is significantly higher than the risk of cell-free infection. For example, the cell-to-cell spread-related infection of HIV-1 is 1.4 times more effective than cell-free infection (Iwami et al., 2015). Cell-to-cell spread of viruses not only accelerates viral dispersion but also has the potential to induce immune evasion (Martin and Sattentau, 2009). For HSV, cell-to-cell spread is also the major infection mode *in vitro* and *in vivo*. There are four main modes of cell-to-cell spread of HSV, namely, cell-cell plasma-membrane fusion, tight junctions, neural synapses and actin-containing or tubulin-containing structures (Sattentau, 2008). Multiple glycoproteins participate in the cell-to-cell spread of HSV, such as gD, gB and gH/gL. In addition to viral entry glycoproteins, gD receptors, viral tegument proteins (UL11, UL16 and UL21), gK and the heterodimer gE/gI also play a crucial role in the cell-to-cell spread-related infection of HSV (Huber et al., 2001; Madavaraju et al., 2020). Recent studies have suggested that PTP1B appears to be required for the cell-to-cell spread of HSV (Carmichael et al., 2018). Strikingly, 4A3 markedly inhibited cell-to-cell spread of HSV (Fig. 3), which may be the main reason why 4A3 exhibited significant therapeutic efficacy in inhibiting HSV infection *in vitro* and *in vivo*.

NAbS can neutralize enveloped viruses mainly by affecting viral attachment or the viral entry process of postattachment (internalization or fusion). For example, mAbS that bind to domain III of dengue virus E glycoprotein exert neutralizing effects mainly at the step of viral attachment (Grill and Roehrig, 2001). In contrast, the mAbS against West Nile virus E16 exert neutralizing effects mainly at a step after viral attachment (Nybakkens et al., 2005). In our study, 4A3 not only affected the process of viral attachment but also affected the viral entry process of post-attachment (Fig. 4).

The interaction between gD and its cellular receptor is regarded to be a crucial step in HSV attachment and fusion processes (Krummenacher et al., 2005; Lu et al., 2014). 4A3 exerts neutralization activity by interfering with the binding of gD to the cellular receptor Nectin-1, and at a low concentration, 4A3 can completely block the binding of gD to Nectin-1 (Fig. 7), indicating that the binding ability of 4A3 to gD is stronger than that of Nectin-1 to gD. Previous studies have shown that mutations of gD residues close to R36, H39 and P221 significantly influence the binding ability of gD to Nectin-1 (Connolly et al., 2005). Some gD residues, including Q27, Y38, H39, Q132, D215 and L220-F223, influence the binding ability of gD to Nectin-1 (Di Giovine et al., 2011). In this study, residues S216 to L220 of gD were found to constitute the key epitope for the binding of 4A3 to gD (Fig. 8); this epitope partially overlaps with the key gD-binding epitope on Nectin-1 (patch2), as previously proposed, and is highly conserved across type-1 and type-2 HSV (Fig. S6). Therefore, 4A3 may influence the binding between gD and Nectin-1 by occupying the key epitope of gD for binding to Nectin-1. gD-specific mAbS have been classified into eight groups of which four, groups I, III, IV and VI, react with different discontinuous antigenic sites (Cairns et al., 2017). Previous studies have demonstrated the group Ia mAbS (such as HD1 and LP2) do not react with denatured forms of gD and show reduced neutralizing activities against HSV mutants containing a nucleotide change in the gD gene which alters residue 216 from asparagine to serine, suggesting that this amino acid might be in the epitope of group Ia mAbS (Lazeal et al., 2012; Minson et al., 1986; Muggeridge et al., 1990). Since group Ia mAbS likely functions by blocking nectin-1 binding, it is reasonable to speculate that 4A3 may recognize a similar epitope with group Ia mAbS. In our study, we found that two critical gD residues, G218 and M219, may influence

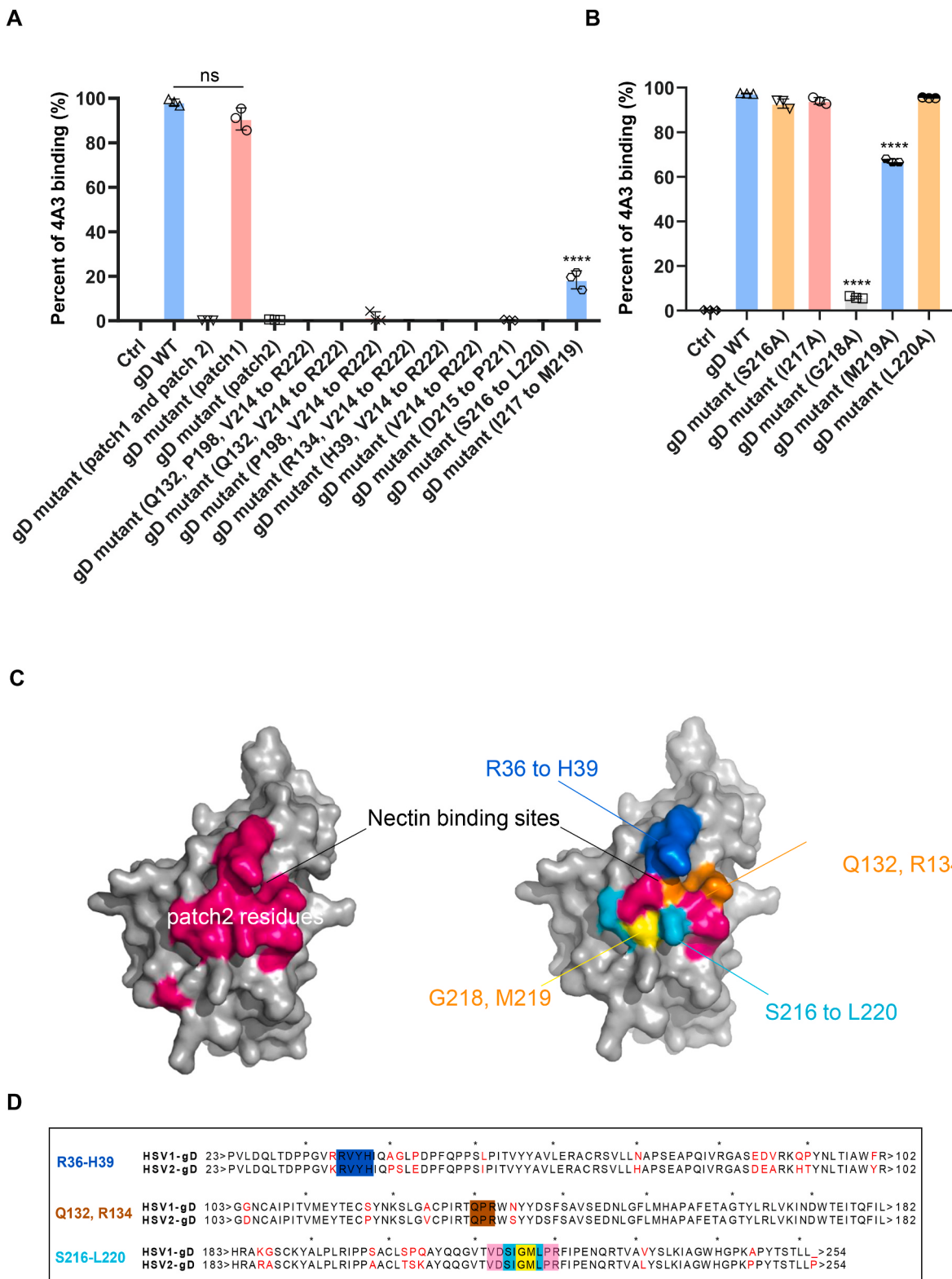


Fig. 8. Detailed epitope mapping of 4A3. (A) The binding of 4A3 to the gD mutants was measured by flow cytometry. (B) The influences of gD mutations (residues S216 to L220) on the binding of 4A3 to gD. (C) The patch 2 residues of the Nectin-1 binding sites on HSV gD2 protein (PDB: 4MYV) are labeled in magenta. The key conserved amino acid residues of 4A3 binding to gD are labeled in yellow. The S216-L220 residues are labeled in yellow and cyan, the R36-H39 residues are labeled in blue, and the Q132 and R134 residues are labeled in orange. (D) Comparison of the amino acids of gD1 and gD2. The different amino acids are highlighted in red font. All the data are presented as the mean \pm SD from at least three independent experiments. Significant differences were analyzed by unpaired two-tailed Student's t-test (A).

the binding ability of gD to 4A3. The mutation at gD residue 216 did not influence the binding ability of 4A3 to gD. Importantly, 4A3 was able to bind to this gD mutant, suggesting that its epitope maybe distinct from that seen by group Ia mAbs. Moreover, because the key epitope of 4A3 is located on the C-terminal extension region (residues 185 to 250) of gD, which can trigger membrane fusion, we speculated that 4A3 would affect the conformational changes of HSV gD, interfering with the subsequent fusion process and thus inhibiting HSV entry.

In summary, we obtained an mAb, termed 4A3, with high cross-neutralizing activity against HSV-1 and HSV-2; 4A3 prevents the cell-to-cell spread of HSV and has a protective effect against HSV-2 infection at lethal doses in BALB/c mice. Furthermore, we found that 4A3 targets a highly conserved continuous epitope on HSV gD, and the neutralization mechanism of 4A3 may involve interference with the binding of gD to Nectin-1, affecting the triggering of membrane fusion and thus inhibiting viral infection. Our findings will promote the development of novel therapeutic antibodies and vaccines against HSV.

Declaration of competing interest

The authors declare that they have no known competing financial interests or personal relationships that could have appeared to influence the work reported in this paper.

Acknowledgments

We thank members of our laboratory for discussions and Dr. Hai Yu for technical assistance. This work was supported by the Science and Technology Program of Xiamen, China [grant number 3502Z20203015].

Appendix A. Supplementary data

Supplementary data to this article can be found online at <https://doi.org/10.1016/j.antiviral.2022.105298>.

References

- Antoine, T.E., Park, P.J., Shukla, D., 2013. Glycoprotein targeted therapeutics: a new era of anti-herpes simplex virus-1 therapeutics. *Rev. Med. Virol.* 23, 194–208.
- Atanasiu, D., Saw, W.T., Cairns, T.M., Eisenberg, R.J., Cohen, G.H., 2021. Using split luciferase assay and anti-HSV glycoprotein monoclonal antibodies to predict a functional binding site between gD and gH/gL. *J. Virol.* 95 (8).
- Awasthi, S., Zumbrun, E.E., Si, H., Wang, F., Shaw, C.E., Cai, M., Lubinski, J.M., Barrett, S.M., Balliet, J.W., Flynn, J.A., Casimiro, D.R., Bryan, J.T., Friedman, H.M., 2012. Live attenuated herpes simplex virus 2 glycoprotein E deletion mutant as a vaccine candidate defective in neuronal spread. *J. Virol.* 86, 4586–4598.
- Belshe, R.B., Leone, P.A., Bernstein, D.I., 2012. Efficacy results of a trial of a herpes simplex vaccine. *N. Engl. J. Med.* 366, 34–43.
- Birkmann, A., Zimmermann, H., 2016. HSV antivirals - current and future treatment options. *Curr Opin Virol* 18, 9–13.
- Boston Interhospital Virus Study, G., Study, N.I.-S.C.A.C., 1975. Failure of high dose 5-iodo-2'-deoxyuridine in the therapy of herpes simplex virus encephalitis. Evidence of unacceptable toxicity. *N. Engl. J. Med.* 292, 599–603.
- Bourne, N., Bravo, F.J., Francotte, M., 2003. Herpes simplex virus (HSV) type 2 glycoprotein D subunit vaccines and protection against genital HSV-1 or HSV-2 disease in Guinea pigs. *J. Infect. Dis.* 187, 542–549.
- Cairns, T.M., Atanasiu, D., Saw, W.T., Lou, H., Whitbeck, J.C., Ditto, N.T., Bruun, B., Browne, H., Bennett, L., Wu, C., Krummenacher, C., Brooks, B.D., Eisenberg, R.J., Cohen, G.H., 2020. Localization of the interaction site of herpes simplex virus glycoprotein D (gD) on the membrane fusion regulator, gH/gL. *J. Virol.* 94.
- Cairns, T.M., Ditto, N.T., Lou, H., Brooks, B.D., Atanasiu, D., Eisenberg, R.J., Cohen, G.H., 2017. Global sensing of the antigenic structure of herpes simplex virus gD using high-throughput array-based SPR imaging. *PLoS Pathog* 13, e1006430.
- Cairns, T.M., Fontana, J., Huang, Z.Y., Whitbeck, J.C., Atanasiu, D., Rao, S., Shelly, S.S., Lou, H., Ponce de Leon, M., Steven, A.C., Eisenberg, R.J., Cohen, G.H., 2014a. Mechanism of neutralization of herpes simplex virus by antibodies directed at the fusion domain of glycoprotein B. *J. Virol.* 88, 2677–2689.
- Cairns, T.M., Huang, Z.Y., Whitbeck, J.C., Ponce de Leon, M., Lou, H., Wald, A., Krummenacher, C., Eisenberg, R.J., Cohen, G.H., 2014b. Dissection of the antibody response against herpes simplex virus glycoproteins in naturally infected humans. *J. Virol.* 88, 12612–12622.
- Campadelli-Fiume, G., Cocchi, F., Menotti, L., Lopez, M., 2000. The novel receptors that mediate the entry of herpes simplex viruses and animal alphaherpesviruses into cells. *Rev. Med. Virol.* 10, 305–319.
- Carmichael, J.C., Yokota, H., Craven, R.C., Schmitt, A., Wills, J.W., 2018. The HSV-1 mechanisms of cell-to-cell spread and fusion are critically dependent on host PTP1B. *PLoS Pathog* 14, e1007054.
- Cena-Diez, R., Vacas-Cordoba, E., Garcia-Broncano, P., de la Mata, F.J., Gomez, R., Maly, M., Munoz-Fernandez, M.A., 2016. Prevention of vaginal and rectal herpes simplex virus type 2 transmission in mice: mechanism of antiviral action. *Int. J. Nanomed.* 11, 2147–2162.
- Chowdhury, S., Naderi, M., Chouljenko, V.N., 2012. Amino acid differences in glycoproteins B (gB), C (gC), H (gH) and L (gL) are associated with enhanced herpes simplex virus type-1 (McKrae) entry via the paired immunoglobulin-like type-2 receptor α . *J. Virol.* 9, 9.
- Clementi, N., Criscuolo, E., Cappelletti, F., 2017. Entry inhibition of HSV1 and 2 protects mice from viral lethal challenge. *Antivir. Res.* 143, 48–61.
- Connolly, S.A., Jackson, J.O., Jarde茨ky, T.S., Longnecker, R., 2011. Fusing structure and function: a structural view of the herpesvirus entry machinery. *Nat. Rev. Microbiol.* 9, 369–381.
- Connolly, S.A., Jarde茨ky, T.S., Longnecker, R., 2021. The structural basis of herpesvirus entry. *Nat. Rev. Microbiol.* 19, 110–121.
- Connolly, S.A., Landsburg, D.J., Carfi, A., Whitbeck, J.C., Zuo, Y., Wiley, D.C., Cohen, G.H., Eisenberg, R.J., 2005. Potential nectin-1 binding site on herpes simplex virus glycoprotein d. *J. Virol.* 79, 1282–1295.
- Corey, L., Langenberg, A.G., Ashley, R., 1999. Recombinant glycoprotein vaccine for the prevention of genital HSV-2 infection: two randomized controlled trials. *Chiron HSV vaccine study group. JAMA* 282, 331–340.
- Corey, L., Wald, A., Patel, R., 2004. Once-daily valacyclovir to reduce the risk of transmission of genital herpes. *N. Engl. J. Med.* 350, 1–20.
- Crill, W.D., Roehrig, J.T., 2001. Monoclonal antibodies that bind to domain III of dengue virus E glycoprotein are the most efficient blockers of virus adsorption to Vero cells. *J. Virol.* 75, 7769–7773.
- Di Giovine, P., Settembre, E.C., Bhargava, A.K., Luftig, M.A., Lou, H., Cohen, G.H., Eisenberg, R.J., Krummenacher, C., Carfi, A., 2011. Structure of herpes simplex virus glycoprotein D bound to the human receptor nectin-1. *PLoS Pathog* 7, e1002277.
- Du, R., Wang, L., Xu, H., Wang, Z., Zhang, T., Wang, M., Ning, Y., Deng, F., Hu, Z., Wang, H., Li, Y., 2017. A novel glycoprotein D-specific monoclonal antibody neutralizes herpes simplex virus. *Antivir. Res.* 147, 131–141.
- Fatahzadeh, M., Schwartz, R.A., 2007. Human herpes simplex virus infections: epidemiology, pathogenesis, symptomatology, diagnosis, and management. *J. Am. Acad. Dermatol.* 57, 737–763.
- Geng, X., Huang, C., Qin, Y., McCombs, J.E., Yuan, Q., Harry, B.L., Palmer, A.E., Xia, N.S., Xue, D., 2012. Hepatitis B virus X protein targets Bcl-2 proteins to increase intracellular calcium, required for virus replication and cell death induction. In: *Proceedings of the National Academy of Sciences of the United States of America*, vol. 109, pp. 18471–18476.
- Heldwein, E.E., Krummenacher, C., 2008. Entry of herpesviruses into mammalian cells. *Cell. Mol. Life Sci.* 65, 1653–1668.
- Huang, C.H., Yuan, Q., Chen, P.J., Zhang, Y.L., Chen, C.R., Zheng, Q.B., Yeh, S.H., Yu, H., Xue, Y., Chen, Y.X., Liu, P.G., Ge, S.X., Zhang, J., Xia, N.S., 2012. Influence of mutations in hepatitis B virus surface protein on viral antigenicity and phenotype in occult HBV strains from blood donors. *J. Hepatol.* 57, 720–729.
- Huber, M.T., Wisner, T.W., Hegde, N.R., Goldsmith, K.A., Rauch, D.A., Roller, R.J., Krummenacher, C., Eisenberg, R.J., Cohen, G.H., Johnson, D.C., 2001. Herpes simplex virus with highly reduced gD levels can efficiently enter and spread between human keratinocytes. *J. Virol.* 75, 10309–10318.
- Iwami, S., Takeuchi, J.S., Nakaoaka, S., Mammano, F., Clavel, F., Inaba, H., Kobayashi, T., Misawa, N., Aihara, K., Koyanagi, Y., Sato, K., 2015. Cell-to-cell infection by HIV contributes over half of virus infection. *Elife* 4.
- James, C., Harfouche, M., Welton, N.J., Turner, K.M., Abu-Raddad, L.J., Gottlieb, S.L., Looker, K.J., 2020. Herpes simplex virus: global infection prevalence and incidence estimates. *Bull. World Health Organ.* 98, 315–329, 2016.
- Johnston, C., Corey, L., 2016. Current concepts for genital herpes simplex virus infection: diagnostics and pathogenesis of genital tract shedding. *Clin. Microbiol. Rev.* 29, 149–161.
- Johnston, C., Koelle, D.M., Wald, A., 2011. HSV-2: in pursuit of a vaccine. *J. Clin. Invest.* 121, 4600–4609.
- Kaufman, H.E., 1962. Clinical cure of herpes simplex keratitis by 5-iodo-2-deoxyuridine. *Proc Soc Exp Biol Med* 109, 251–252.
- Kimberlin, D.W., Whitley, R.J., Wan, W., 2011. Oral acyclovir suppression and neurodevelopment after neonatal herpes. *N. Engl. J. Med.* 365, 1284–1292.
- Knipe, D.M., Cliffe, A., 2008. Chromatin control of herpes simplex virus lytic and latent infection. *Nat. Rev. Microbiol.* 6, 211–221.
- Koelle, D.M., Corey, L., 2003. Recent progress in herpes simplex virus immunobiology and vaccine research. *Clin. Microbiol. Rev.* 16, 96–113.
- Koelle, D.M., Corey, L., 2008. Herpes simplex: insights on pathogenesis and possible vaccines. *Annu. Rev. Med.* 59, 381–395.
- Krawczyk, A., Arndt, M.A., Grosse-Hovest, L., Weichert, W., Giebel, B., Dittmer, U., Hengel, H., Jager, D., Schneweis, K.E., Eis-Hubinger, A.M., Roggendorf, M., Krauss, J., 2013. Overcoming drug-resistant herpes simplex virus (HSV) infection by a humanized antibody. *Proc. Natl. Acad. Sci. U. S. A.* 110, 6760–6765.
- Krawczyk, A., Krauss, J., Eis-Hubinger, A.M., Daumer, M.P., Schwarzenbacher, R., Dittmer, U., Schneweis, K.E., Jager, D., Roggendorf, M., Arndt, M.A., 2011. Impact of valency of a glycoprotein B-specific monoclonal antibody on neutralization of herpes simplex virus. *J. Virol.* 85, 1793–1803.

- Krummenacher, C., Supekar, V.M., Whitbeck, J.C., Lazear, E., Connolly, S.A., Eisenberg, R.J., Cohen, G.H., Wiley, D.C., Carfi, A., 2005. Structure of unliganded HSV gD reveals a mechanism for receptor-mediated activation of virus entry. *EMBO J* 24, 4144–4153.
- Lathey, J.L., Rouse, B.T., Wiley, D.E., Courtney, R.J., 1986. Production and characterization of an anti-idiotypic antibody specific for a monoclonal antibody to glycoprotein D of herpes simplex virus. *Immunology* 57, 29–35.
- Lazear, E., Whitbeck, J.C., Ponce-de-Leon, M., Cairns, T.M., Willis, S.H., Zuo, Y., Krummenacher, C., Cohen, G.H., Eisenberg, R.J., 2012. Antibody-induced conformational changes in herpes simplex virus glycoprotein gD reveal new targets for virus neutralization. *J. Virol.* 86, 1563–1576.
- Lu, G., Zhang, N., Qi, J., Li, Y., Chen, Z., Zheng, C., Gao, G.F., Yan, J., 2014. Crystal structure of herpes simplex virus 2 gD bound to nectin-1 reveals a conserved mode of receptor recognition. *J. Virol.* 88, 13678–13688.
- Luo, Y., Lin, C., Zou, Y., Ju, F., Ren, W., Lin, Y., Wang, Y., Huang, X., Liu, H., Yu, Z., Liu, P., Tan, G., Yuan, Q., Zhang, J., Huang, C., Xia, N., 2020. Tumor-targeting oncolytic virus elicits potent immunotherapeutic vaccine responses to tumor antigens. *Oncolimmunology* 9, 1726168.
- Luo, Y., Xiong, D., Li, H.H., Qiu, S.P., Lin, C.L., Chen, Q., Huang, C.H., Yuan, Q., Zhang, J., Xia, N.S., 2016. Development of an HSV-1 neutralization test with a glycoprotein D specific antibody for measurement of neutralizing antibody titer in human sera. *J. Virol.* 13, 44.
- Madavaraju, K., Koganti, R., Volety, I., Yadavalli, T., Shukla, D., 2020. Herpes simplex virus cell entry mechanisms: an update. *Front Cell Infect. Microbiol.* 10, 617578.
- Martin, N., Sattentau, Q., 2009. Cell-to-cell HIV-1 spread and its implications for immune evasion. *Curr. Opin. HIV AIDS* 4, 143–149.
- Miller, C.G., Krummenacher, C., Eisenberg, R.J., Cohen, G.H., Fraser, N.W., 2001. Development of a syngenic murine B16 cell line-derived melanoma susceptible to destruction by neuroattenuated HSV-1. *Mol. Ther.* 3, 160–168.
- Minson, A.C., Hodgman, T.C., Digard, P., Hancock, D.C., Bell, S.E., Buckmaster, E.A., 1986. An analysis of the biological properties of monoclonal antibodies against glycoprotein D of herpes simplex virus and identification of amino acid substitutions that confer resistance to neutralization. *J. Gen. Virol.* 67 (Pt 6), 1001–1013.
- Muggeridge, M.I., Wilcox, W.C., Cohen, G.H., Eisenberg, R.J., 1990. Identification of a site on herpes simplex virus type 1 glycoprotein D that is essential for infectivity. *J. Virol.* 64, 3617–3626.
- Nybakken, G.E., Oliphant, T., Johnson, S., Burke, S., Diamond, M.S., Fremont, D.H., 2005. Structural basis of West Nile virus neutralization by a therapeutic antibody. *Nature* 437, 764–769.
- Parr, M.B., Keppler, L., McDermott, M.R., Drew, M.D., Bozzola, J.J., Parr, E.L., 1994. A mouse model for studies of mucosal immunity to vaginal infection by herpes simplex virus type 2. *Lab. Invest.* 70, 369–380.
- Poole, C.L., Kimberlin, D.W., 2018. Antiviral approaches for the treatment of HSV infections in newborn infants. *Annu. Rev. Virol.* 5, 407–425.
- Sattentau, Q., 2008. Avoiding the void: cell-to-cell spread of human viruses. *Nat. Rev. Microbiol.* 6, 815–826.
- Sherwood, J.K., Zeitlin, L., Whaley, K.J., Cone, R.A., Saltzman, M., 1996. Controlled release of antibodies for long-term topical passive immunoprotection of female mice against genital herpes. *Nat. Biotechnol.* 14, 468–471.
- Shukla, D., Spear, P.G., 2001. Herpesviruses and heparan sulfate: an intimate relationship in aid of viral entry. *J. Clin. Invest.* 108, 503–510.
- Steiner, I., 1996. Human herpes viruses latent infection in the nervous system. *Immunol. Rev.* 152, 157–173.
- Turner, A., Bruun, B., Minson, T., Browne, H., 1998. Glycoproteins gB, gD, and gH/gL of herpes simplex virus type 1 are necessary and sufficient to mediate membrane fusion in a cos cell transfection system. *J. Virol.* 72, 873–875.
- Wang, S., Long, J., Zheng, C.F., 2012. The potential link between PML NBs and ICP0 in regulating lytic and latent infection of HSV-1. *Protein Cell* 3, 372–382.
- Whitley, R.J., Roizman, B., 2001. Herpes simplex virus infections. *Lancet* 357, 1513–1518.